Inactive

RM No. L7J17
Copy No. 4

NACA

26 NOV 1947

RESEARCH MEMORANDUM

for the

Air Materiel Command, Army Air Forces

INVESTIGATION OF THE STABILITY AND CONTROL CHARACTERISTICS OF A $\frac{1}{20}$-SCALE MODEL OF THE CONSOLIDATED VULTEE XB-53 AIRPLANE IN THE LANGLEY FREE-FLIGHT TUNNEL

By

Charles V. Bennett

Langley Memorial Aeronautical Laboratory
Langley Field, Va.

NATIONAL ADVISORY COMMITTEE FOR AERONAUTICS

RESEARCH MEMORANDUM

for the

Air Materiel Command, Army Air Forces

INVESTIGATION OF THE STABILITY AND CONTROL CHARACTERISTICS OF A $\frac{1}{20}$-SCALE MODEL OF THE CONSOLIDATED VULTEE XB-53 AIRPLANE IN THE LANGLEY FREE-FLIGHT TUNNEL

By Charles V. Bennett

SUMMARY

An investigation of the low-speed, power-off stability and control characteristics of a $\frac{1}{20}$-scale model of the Consolidated Vultee XB-53 airplane has been conducted in the Langley free-flight tunnel. In the investigation it was found that with flaps neutral satisfactory flight behavior at low speeds was obtainable with an increase in height of the vertical tail and with the inboard slats opened. In the flap-down slat-open condition the longitudinal stability was satisfactory, but it was impossible to obtain satisfactory lateral-flight characteristics even with the increase in height of the vertical tail because of the negative effective dihedral, low directional stability, and large adverse yawing moments of the ailerons.

INTRODUCTION

An investigation of the low-speed, power-off stability and control characteristics of a $\frac{1}{20}$-scale model of the Consolidated Vultee XB-53 airplane has been conducted in the Langley free-flight tunnel at the request of the Air Materiel Command, Army Air Forces. The XB-53 is a jet-propelled, sweptforward, tailless bomber design.

The present investigation included force and flight tests of the $\frac{1}{20}$-scale model without power for both the flap-retracted and flap-extended configurations.

SYMBOLS

S	wing area, square feet
$\bar{c}$	mean aerodynamic chord, feet
b	wing span, feet
q	dynamic pressure, pounds per square foot
ρ	air density, slugs per cubic foot
α	angle of attack, degrees
β	angle of sideslip, degrees
δ_a	aileron deflection, degrees
C_L	lift coefficient (Lift/qS)
C_D	drag coefficient (Drag/qS)
C_m	pitching-moment coefficient (Pitching moment/$qS\bar{c}$)
C_n	yawing-moment coefficient (Yawing moment/qSb)
C_l	rolling-moment coefficient (Rolling moment/qSb)
C_Y	lateral-force coefficient (Lateral force/qS)
C_{Y_β}	rate of change of lateral-force coefficient with angle of sideslip, per degree $\left(\partial C_Y/\partial\beta\right)$
C_{n_β}	rate of change of yawing-moment coefficient with angle of sideslip, per degree $\left(\partial C_n/\partial\beta\right)$
C_{l_β}	rate of change of rolling-moment coefficient with angle of sideslip, per degree $\left(\partial C_l/\partial\beta\right)$

Subscripts:

l	left
r	right

[redacted]

APPARATUS

Wind Tunnel

The investigation was made in the Langley free-flight tunnel which was designed to test free-flying dynamic models. A complete description of the tunnel and its operation is given in reference 1.

The force tests to determine the static aerodynamic characteristics of the model were made on the free-flight-tunnel six-component balance which is described in reference 2. This balance rotates in yaw with the model such that all forces and moments are measured with respect to the stability axes. A sketch showing the positive direction of the forces and moments and the definition of the stability axes is given in figure 1.

Model

The $\frac{1}{20}$-scale model used in the investigation was constructed at the Langley Laboratory. A three-view drawing of the model is presented in figure 2 and photographs of the model are given as figure 3. Table I gives the dimensional and mass characteristics of the full-scale design and the scaled-up dimensional and mass characteristics of the model. It was impossible to duplicate the scaled-down moments of inertia on the $\frac{1}{20}$-scale model because of the weight distribution of the materials used in the construction. A rough check of some of the estimated moments of inertia for the full-scale airplane indicates that the estimated values are probably low. The moments of inertia of the free-flight-tunnel model, therefore, are probably not as much greater than the airplane scale-down values as appears in table I.

The wing of the model has a Rhode St. Genese 35 airfoil section perpendicular to the 0.50 chord line. The substitution of this section for that specified for the full-scale design (NACA 65_1-012) was in accordance with free-flight-tunnel practice of using airfoil sections which obtain maximum lift coefficients in the low-scale tests more nearly equal to those of the full-scale airplane using the design airfoil.

For the flap-down configuration on the airplane, an outboard single-slotted flap with trailing-edge aileron is deflected and an inboard leading-edge slat is extended. (See fig. 4.) For the free-flight-tunnel tests, the inboard leading-edge slat was also used with the flap-retracted

[redacted]

configuration in an effort to improve the longitudinal and directional stability at high-lift coefficients.

The model was modified for some of the tests by adding an extension to the design vertical tail as shown in figure 2.

TESTS

Force Tests

All force tests were made in the Langley free-flight tunnel at a dynamic pressure of 3.0 pounds per square foot which corresponds to about 34 miles per hour at standard sea-level conditions and to a test Reynolds number of 309,000 based on the mean aerodynamic chord of 0.961 foot.

Force tests were made to determine the lift, drag, and pitching-moment characteristics of the model with the flap retracted and flaps extended with the leading-edge slat on and off for an angle-of-attack range from -8° to 20°. Because of the camber of the airfoil used on the model, it was necessary that the elevators and ailerons be deflected -10° so as to give about the same basic pitching moment as the airplane with its design airfoil.

Force tests were made over an angle-of-attack range of $\pm 5^\circ$ yaw to determine the lateral stability characteristics of the model with the vertical tail off, with the design vertical tail on, and with an extension on the design vertical tail. Tests were also made to determine the effect of the leading-edge slats on the lateral stability characteristics for both the flap-retracted and flap-extended configurations.

Aileron-effectiveness tests were made with flaps down over an angle-of-attack range with the ailerons deflected up and down 20° and up 40° from the zero neutral position.

Flight Tests

Flight tests with flap retracted were made with the leading-edge slat on and off over a lift-coefficient range from $C_L = 0.44$ to $C_L = 0.83$. In addition, some tests were made with an extension on the design vertical tail.

In the flap-extended configurations, all flight tests were made with the leading-edge slat on. In addition to the tests with the design

vertical tail, a few tests were made with an extension on the tail. Tests with the flap extended were made over a lift-coefficient range from $C_L = 0.48$ to $C_L = 0.98$.

RESULTS AND DISCUSSION

Force Tests

The results of force tests made to determine the longitudinal and lateral stability characteristics of the free-flight-tunnel model are presented in figures 5 to 11. Comparable data from reference 3 obtained from higher speed tests (Reynolds number = 2,430,000) of a $\frac{1}{10}$-scale model at GALCIT (Guggenheim Aeronautical Laboratory, California Institute of Technology) are also presented on these figures. All free-flight-tunnel data are referred to the normal center-of-gravity location at 9.8 percent of the mean aerodynamic chord and all GALCIT data presented are referred to a center-of-gravity location of 11 percent of the mean aerodynamic chord.

Flap retracted.—The longitudinal stability data of figure 5 indicate that the free-flight-tunnel results for the flap-retracted configuration were generally in good agreement with the higher scale GALCIT tests except for the greater reduction in longitudinal stability at the stall for the free-flight-tunnel model. This difference is probably caused by the difference in the scale of the tests. With the leading-edge slat extended, however, the pitching-moment curve for the free-flight-tunnel model remained stable at the stall (fig. 6) and was, in this respect, in agreement with the GALCIT results without the slat. It is believed, therefore, that the longitudinal stability of the free-flight-tunnel model at the stall with slat on will be representative of the airplane with slat off. The static margin was slightly reduced over the lift range up to the stall by the addition of the slat.

Flap-retracted lateral-stability data for the free-flight model are presented in figure 7 along with the GALCIT data. The data are presented in the form of plots of the stability parameters C_{n_β}, C_{l_β}, and C_{Y_β} against angle of attack. These data indicate decreasing positive effective dihedral up to the stall, at which point the effective dihedral increased rapidly. The same general variation of effective dihedral with angle of attack was shown for both the free-flight and GALCIT models.

[redacted]

The data of figure 7 indicate about the same directional stability over the angle-of-attack range for both the free-flight and GALCIT models with slat retracted. A serious decrease in the directional stability occurred above an angle of attack of about 12° for both models. The addition of the leading-edge slat to the free-flight-tunnel model eliminated this decrease in directional stability at high angles of attack but reduced the directional stability somewhat at lower angles of attack.

Flap and slat extended.- The longitudinal stability data of figure 8 indicate good agreement between the GALCIT and free-flight-tunnel tests for the configurations with flap down and leading-edge slat extended. Both sets of data indicate a nosing down (stable) tendency at the stall.

The lateral stability data presented in figure 9 show that the effective dihedral C_{l_β} for both models is slightly negative at low angles of attack and increases negatively up to the stall, at which point the effective dihedral becomes positive.

The data of figure 9 also indicate that the directional stability for both models with the leading-edge slat off is low at the lower lift coefficients and decreases to the point of instability at high lift coefficients. Since poor flying characteristics were anticipated because of the low directional stability, an extension was added to the vertical tail (fig. 2) and data presented in figure 9 show that the extension increased the directional stability so that positive directional stability was obtained throughout the lift range. Test data obtained with the leading-edge slat on are also presented in figure 9 and show that the slat greatly increased the directional stability at high lift coefficients.

The data of figures 7 and 9 have been summarized in figure 10 in the form of a lateral-stability chart. The slat-off data of figure 10(a) show the large reduction in effective dihedral when the flaps are deflected 30° and also the reduction in directional stability at the higher angles of attack. The addition of the leading-edge slat (fig. 10(b)) reduced the large change in effective dihedral with flap deflection and also reduced the change in directional stability with angle of attack.

Data showing the rolling and yawing moments produced by the ailerons of the GALCIT and free-flight models are shown in figure 11. The rolling effectiveness of the ailerons on the free-flight-tunnel model is less than that shown for the GALCIT model for the flap-down configuration. This is attributed in part to the gap seal on the flaps of the free-flight model which was used because of the difficulty encountered in keeping the gap constant during the model flight tests. Force-test data (not presented) showed that the downgoing aileron on the free-flight-tunnel model with flap down was almost ineffective, which accounted for most

[redacted]

of the difference in the aileron effectiveness of the GALCIT and free-flight models. Rolling moments obtained with one aileron up 40° were somewhat greater than those obtained with ±20° deflection on the free-flight model but were still less than those of the GALCIT model with ±20° deflection. The adverse yawing moments due to aileron deflections of ±20° for the GALCIT model are shown to increase with flap deflection and lift coefficient and are greater than those of the free-flight model with flaps deflected. When one aileron was deflected up 40°, only small adverse yaw was obtained at the lower lift coefficients and favorable yaw was obtained above a lift coefficient of 0.75.

Flight Tests

Flap retracted.- The flight tests made with the flap retracted, with the design vertical tail, and with the leading-edge slat off showed fairly satisfactory longitudinal and lateral flight characteristics at lift coefficients between 0.44 and 0.65. At these moderate lift coefficients, however, more directional stability was desirable, especially when flights were made with the ailerons as the sole means of lateral control, because of objectionable adverse yawing. Flight tests indicated that large amounts of rudder control (about ±10°) were necessary to overcome the adverse yawing. Above a lift coefficient of 0.65 there was considerable yawing motion of the model accompanied at times by a nosing-up tendency which often resulted in the model going out of control and crashing. Increasing the directional stability by adding an extension on the vertical tail was beneficial in that it delayed the onset of poor stability conditions to a slightly higher lift coefficient, but this did not reduce the severity of the instability at the stall. The nosing-up tendency (fig. 5) at the stall appeared to be aggravated by the adverse yawing, and the combination of these two characteristics resulted in very erratic flight conditions as the stall was approached.

The addition of the inboard leading-edge slat made the longitudinal stability satisfactory at the stall and it appears, therefore, that the longitudinal stability of the airplane with the slat closed might be satisfactory since higher-scale force tests (GALCIT) indicated that the airplane with slat off will have about the same static longitudinal stability at the stall as the free-flight-tunnel model with slat on. The slat was also effective in improving directional stability at high angles of attack and resulted in the directional stability being maintained to a higher lift coefficient which provided better flight behavior up to $C_L = 0.83$ although the yawing motions were still unsatisfactory. (This improvement in flight characteristics would be expected from the force-test data of figs. 6 and 7.)

[redacted]

Since the data for both the free-flight and GALCIT models indicate a need for the leading-edge slat to improve the directional stability at the stall, it appears that a slat will be required for the airplane even though it is not necessary from the standpoint of longitudinal stability.

Flap extended.- The results of the flight tests of the model in the flap-extended configuration indicated no serious longitudinal-stability difficulties for the lift-coefficient range tested ($C_L = 0.44$ to $C_L = 0.98$).

The model had poor lateral-flight characteristics because of the low directional stability and the large amount of negative dihedral (fig. 9) and it was necessary to increase the rudder deflection from $\pm 10^\circ$ to $\pm 18^\circ$ to overcome the adverse yaw of the ailerons. With the increased rudder travel, flights with combined aileron and rudder control were fairly good. Flights were very difficult to maintain, however, when the ailerons were used as the sole means of lateral control. This was attributed to the large adverse yawing moment due to the ailerons shown for the flap-extended configuration in figure 11 and to the probable large adverse yaw due to rolling for this design. Large adverse yawing moments due to the ailerons are characteristic of this aileron-flap arrangement as shown by full-scale tests reported in reference 4.

The increased directional stability afforded by the extension added to the vertical tail was helpful in improving the lateral flying characteristics to the extent that less attention to the lateral control was required of the pilot when coordinated ailerons and rudder were used. Even with the extended vertical tail, however, flights with aileron alone were unsatisfactory because the application of aileron control caused the model to yaw adversely and when the yaw became large the negative effective dihedral caused the leading wing to "dig in" resulting in the model slipping off and crashing into the tunnel wall.

Flights made with ailerons alone when the ailerons were deflected 40° in only the up direction indicated some improvement in the flying characteristics because, with the decreased adverse aileron yawing moments, the yawing motion did not build up so rapidly. The yawing motion, however, eventually did build up until the model went out of control.

CONCLUDING REMARKS

The results of the free-flight-tunnel stability and control investigation of the $\frac{1}{20}$-scale model of the Consolidated Vultee XB-53 airplane may be summarized as follows:

[redacted]

Flap retracted:

1. The model was longitudinally unstable at the stall without the slat but was stable with the slat on. The airplane might be satisfactory longitudinally since higher scale tests indicate that the airplane with slat off will have the same static longitudinal stability at the stall as the model had with slat on.

2. The directional stability afforded by the design vertical tail was low and dropped off sharply at the stall, which resulted in poor lateral-flight characteristics at the higher lift coefficients. The vertical-tail extension improved the directional stability, but it was still unsatisfactory at high lift coefficients.

3. The addition of the leading-edge slat eliminated the sharp drop in directional stability at high angles of attack.

Flap extended and leading-edge slat open:

1. The longitudinal stability was satisfactory throughout the lift range tested.

2. The directional stability was insufficient either with the design vertical tail or with the vertical-tail extension added.

3. The design flap-aileron arrangement gave large adverse yawing moments due to aileron deflection.

4. The large negative effective dihedral, together with the low directional stability and adverse yaw due to ailerons, resulted in very poor lateral stability characteristics even with the vertical tail extension added.

RECOMMENDATIONS

The following recommendations for improving the stability characteristics of the XB-53 airplane are made on the basis of the results obtained in the free-flight-tunnel investigation:

1. The use of a larger, higher aspect ratio vertical tail and an inboard leading-edge slat would probably make the flap-up configuration fairly satisfactory.

2. Increasing the directional stability by using a larger vertical tail would also be beneficial for the flap-down configuration, but it is extremely unlikely that even the largest vertical tail which could reasonably be used on the airplane would make it satisfactory.

[redacted]

The outboard slotted flap with the trailing-edge aileron seems to be the source of the flap-down trouble, and the difficulty might be remedied by the use of some other high-lift device and another type of lateral control which would reduce both the adverse yaw due to aileron deflection and the negative effective dihedral.

Langley Memorial Aeronautical Laboratory
National Advisory Committee for Aeronautics
Langley Field, Va.

Charles V. Bennett

Charles V. Bennett
Aeronautical Engineer

Approved:

Thomas A. Harris

Thomas A. Harris
Chief of Stability Research Division

KBC

REFERENCES

1. Shortal, Joseph A., and Osterhout, Clayton J.: Preliminary Stability and Control Tests in the NACA Free-Flight Wind Tunnel and Correlation with Full-Scale Flight Tests. NACA TN No. 810, 1941.

2. Shortal, Joseph A., and Draper, John W.: Free-Flight-Tunnel Investigation of the Effect of the Fuselage Length and the Aspect Ratio and Size of the Vertical Tail on Lateral Stability and Control. NACA ARR No. 3D17, 1943.

3. Anon.: Summary Report, Tests of 1/10-Scale XB-53 Complete Model, GALCIT 10-Ft. Tunnel Rep. No. FZT-112-007, Consolidated Vultee Aircraft Corp., Dec. 16, 1946.

4. Sawyer, Richard H.: Flight Measurements of the Lateral Control Characteristics of Narrow-Chord Ailerons on the Trailing Edge of a Full-Span Slotted Flap. NACA TN No. 1188, 1947.

[redacted]

TABLE I

DIMENSIONAL AND MASS CHARACTERISTICS OF THE XB-53

	Scaled-Up	Full-Scale
Weight, lb	51,456	60,211
Relative density factor (m/ρSb)	6.475	7.585
Wing:		
Area, sq ft	1380.0	1380.0
Span, ft	75.07	75.07
Aspect ratio	4.00	4.00
Sweepforward, 0.25 chord line	30.0	30.0
Dihedral, deg	7.0	7.0
Mean aerodynamic chord, ft	19.25	19.25
Root chord, ft	24.75	24.75
Tip chord, ft	12.375	12.375
Wing loading, W/S, lb/sq ft	37.3	43.7
Airfoil	Rhode St. Genese 35	NACA 65_1-012
Vertical Tail:		
Design, area, sq ft	135.0	135.0
Extended, area, sq ft	155.5	- - -
Center-of-gravity location, percent M.A.C.	9.8	9.8
Moment of inertia:		
Full-load condition		
I_x, lb-ft^2	[a]6,906,000	9,407,000
I_y, lb-ft^2	[a]18,428,000	7,593,000
I_z, lb-ft^2	[a]26,139,000	16,981,000
Empty condition:		
I_x, lb-ft^2	(Impossible to ballast model to this condition.)	3,343,000
I_y, lb-ft^2		6,241,000
I_z, lb-ft^2		9,572,000

[a]Free-flight-model tests were made at inertia values of between ±10 percent of scaled-up listed values.

NACA

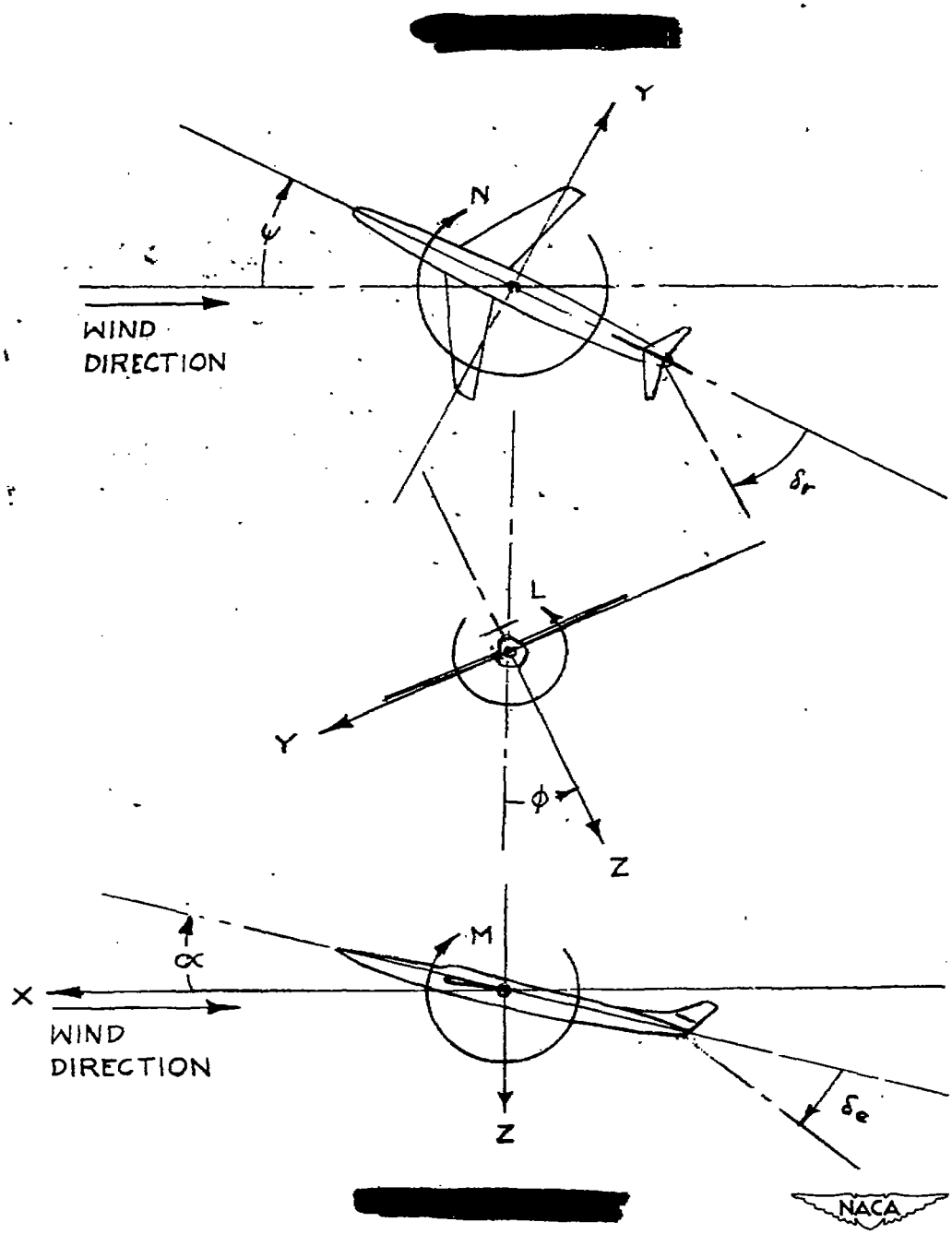

Figure 1.- The stability system of axes. Arrows indicate positive directions of moments, forces, and control-surface deflections. This system of axes is defined as an orthogonal system having their origin at the center of gravity and in which the Z-axis is in the plane of symmetry and perpendicular to the relative wind, the X-axis is in the plane of symmetry and perpendicular to the Z-axis, and the Y-axis is perpendicular to the plane of symmetry.

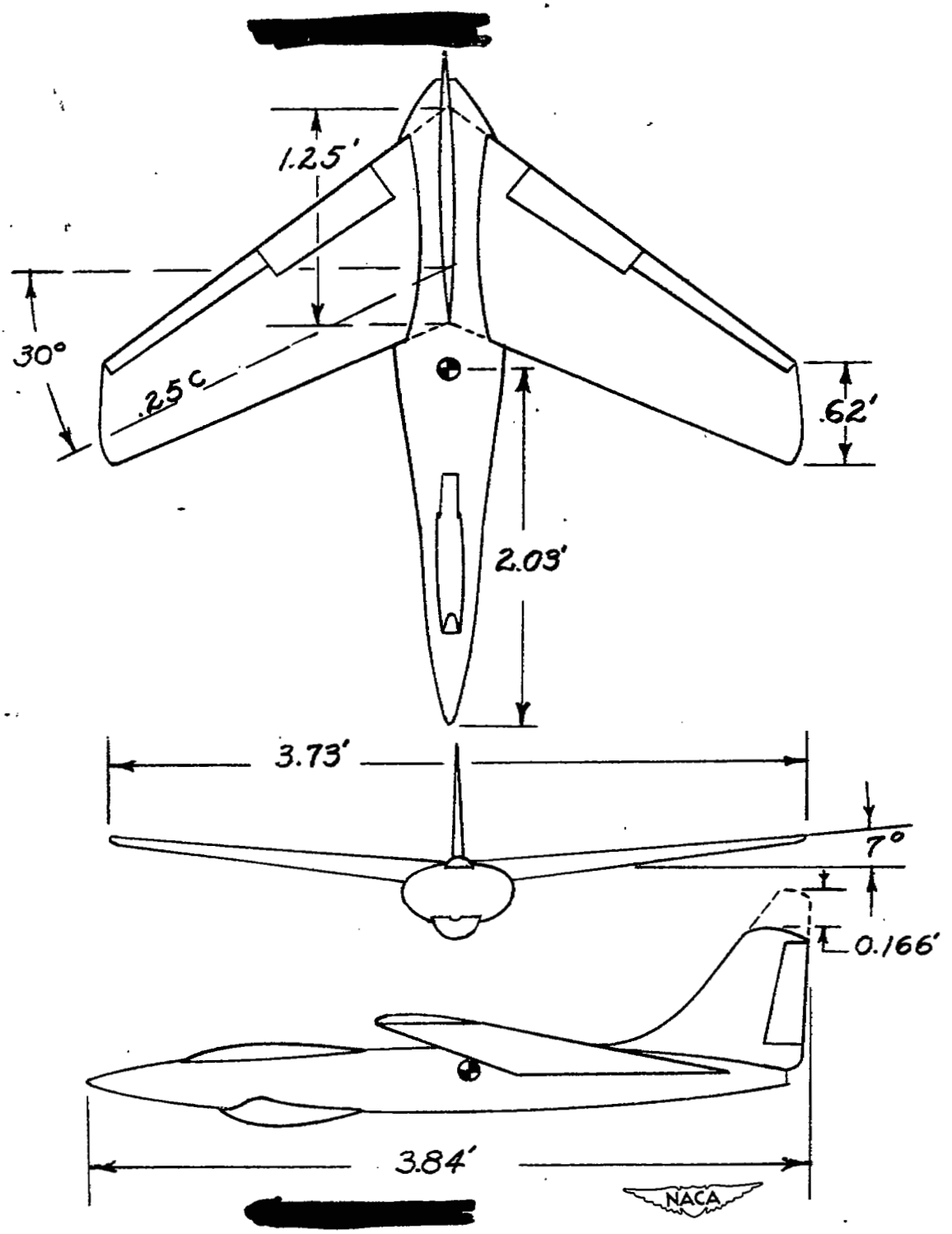

Figure 2.- Three-view sketch of the $\frac{1}{20}$-scale model of the Consolidated Vultee XB-53 airplane tested in the Langley free-flight tunnel.

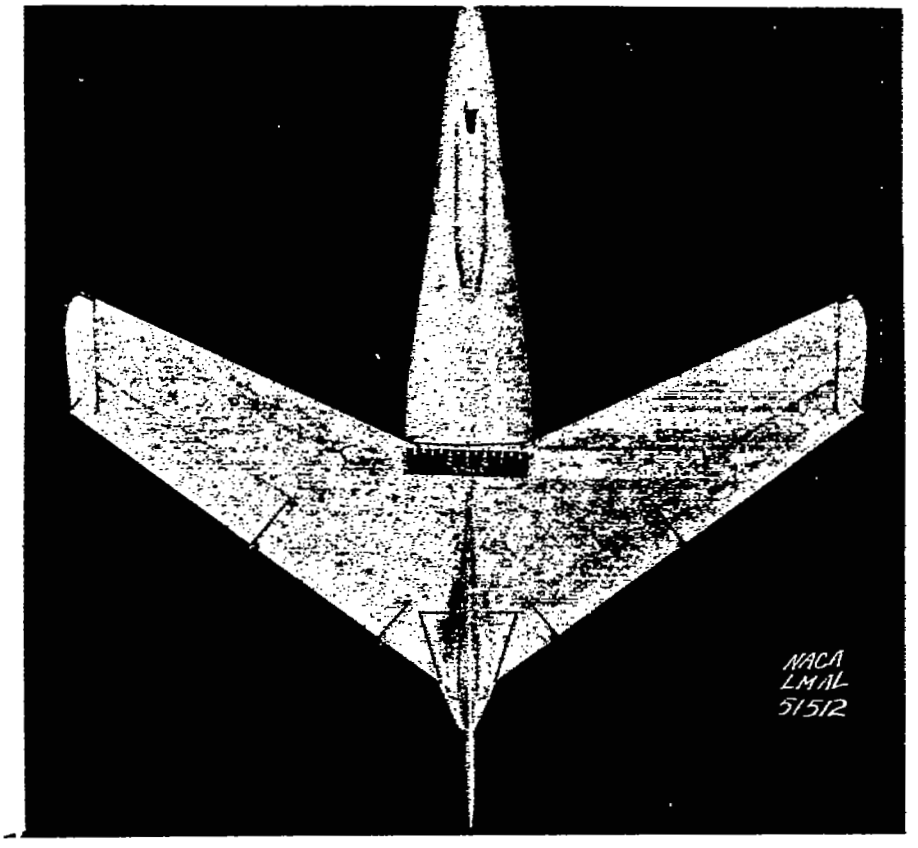

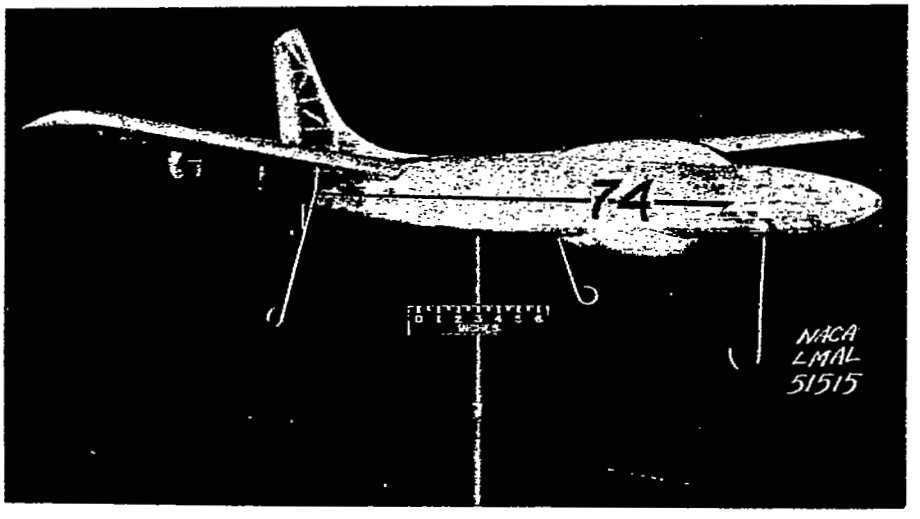

Figure 3.- Photographs of $\frac{1}{20}$-scale model of the Consolidated Vultee XB-53 airplane.

NATIONAL ADVISORY COMMITTEE FOR AERONAUTICS
LANGLEY MEMORIAL AERONAUTICAL LABORATORY - LANGLEY FIELD, VA.

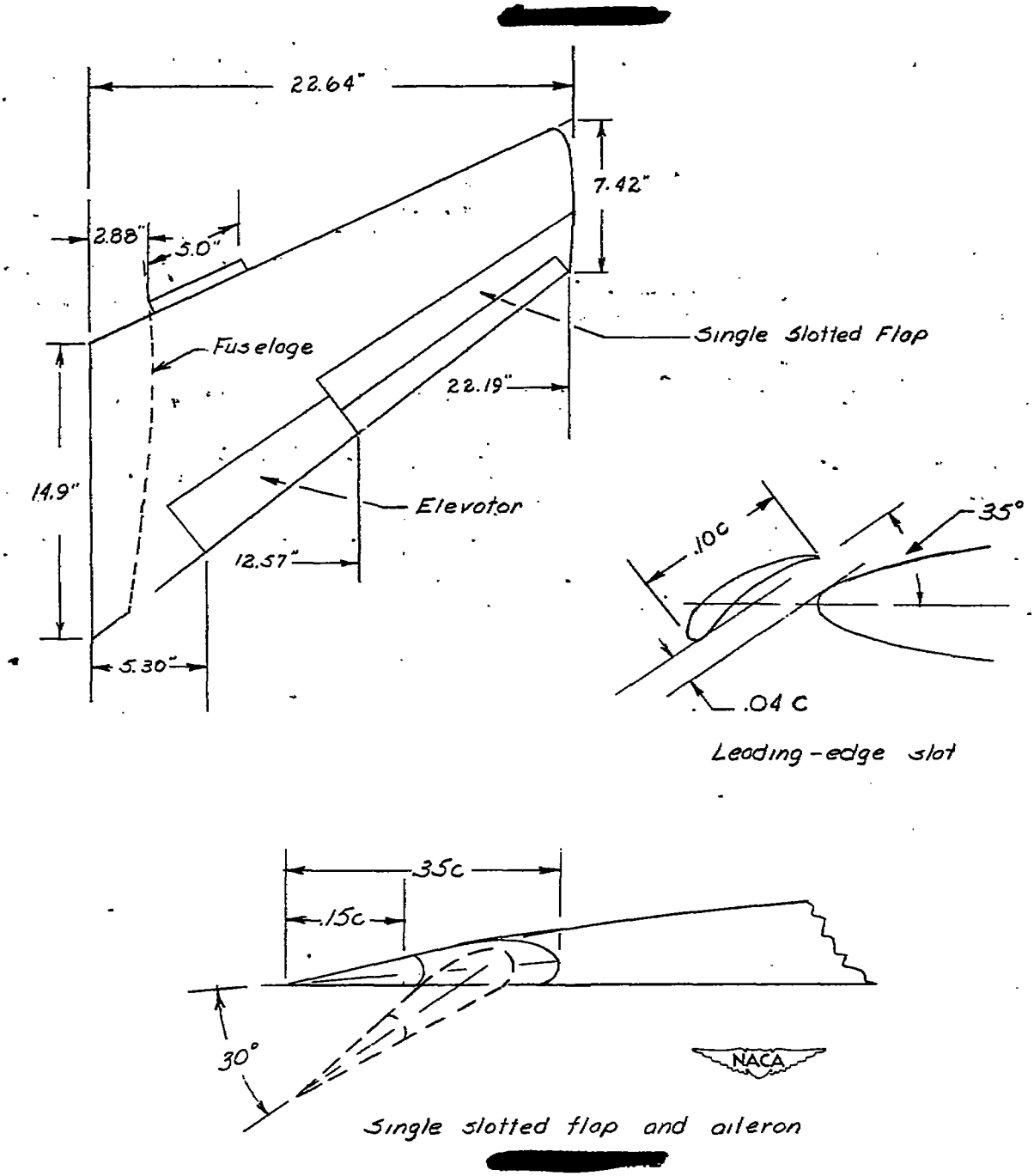

Figure 4.- Leading-edge slat and single slotted flap arrangement tested in the free-flight-tunnel investigation of the stability and control characteristics of a $\frac{1}{20}$-scale model of the Consolidated Vultee XB-53 airplane.

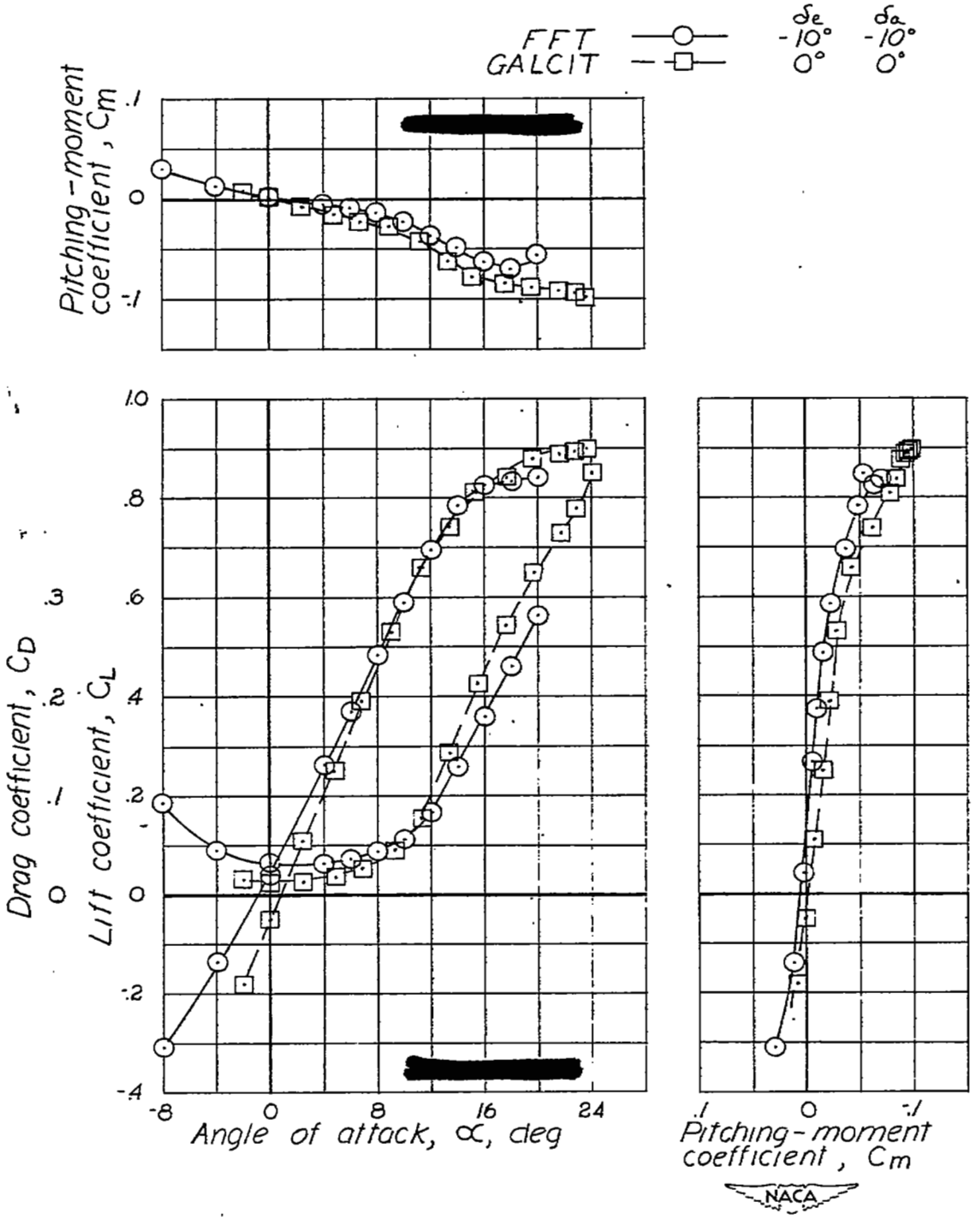

Figure 5.- Lift, drag, and pitching-moment characteristics of the $\frac{1}{20}$-scale free-flight-tunnel model of the Consolidated Vultee XB-53 airplane compared with the $\frac{1}{10}$-scale GALCIT model. Flaps retracted. GALCIT data from reference 3. Leading-edge slat off.

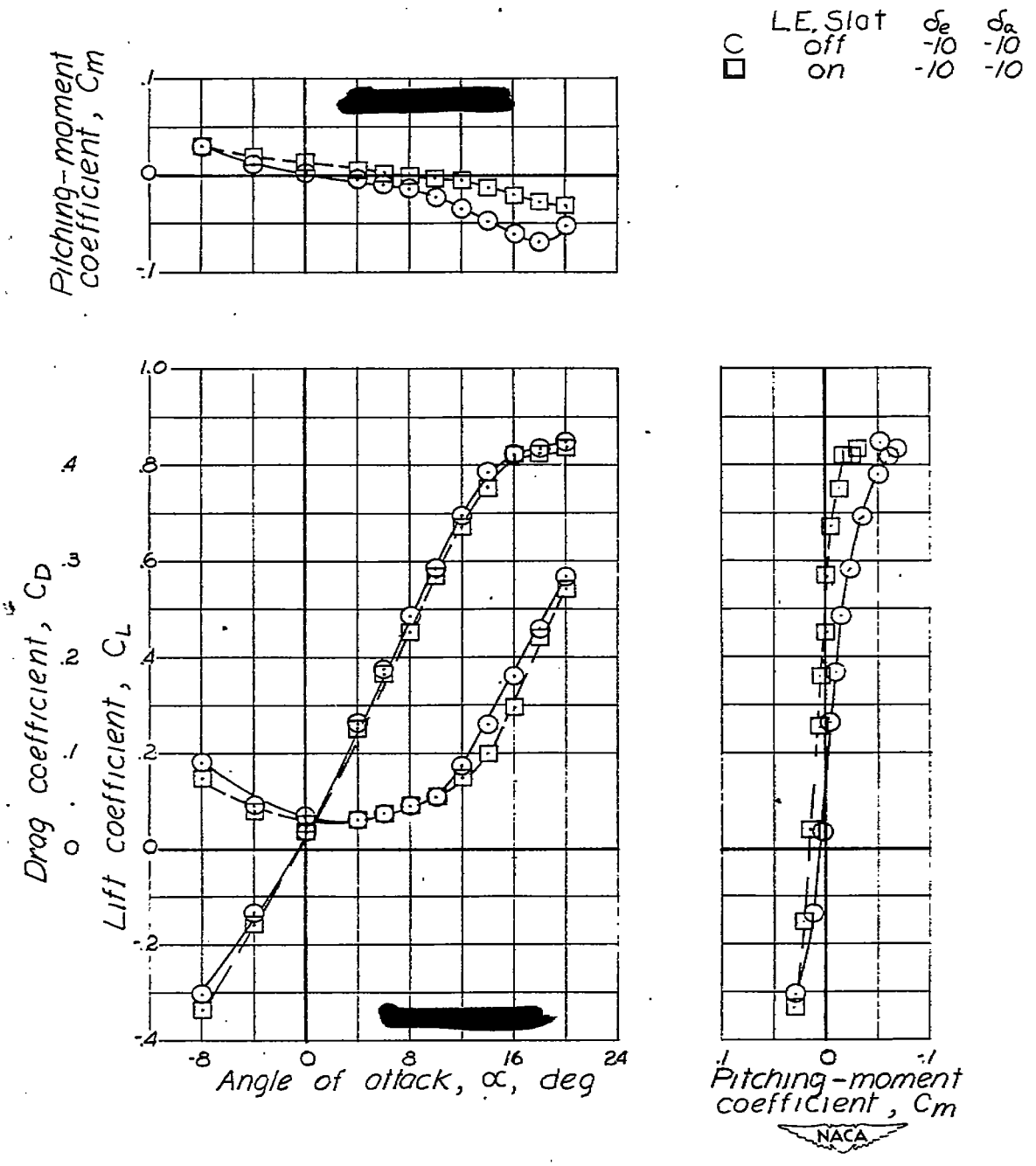

Figure 6.- Effect of leading-edge slat on the lift, drag, and pitching-moment characteristics of the Langley free-flight-tunnel $\frac{1}{20}$-scale model of the Consolidated Vultee XB-53 airplane. Flaps retracted.

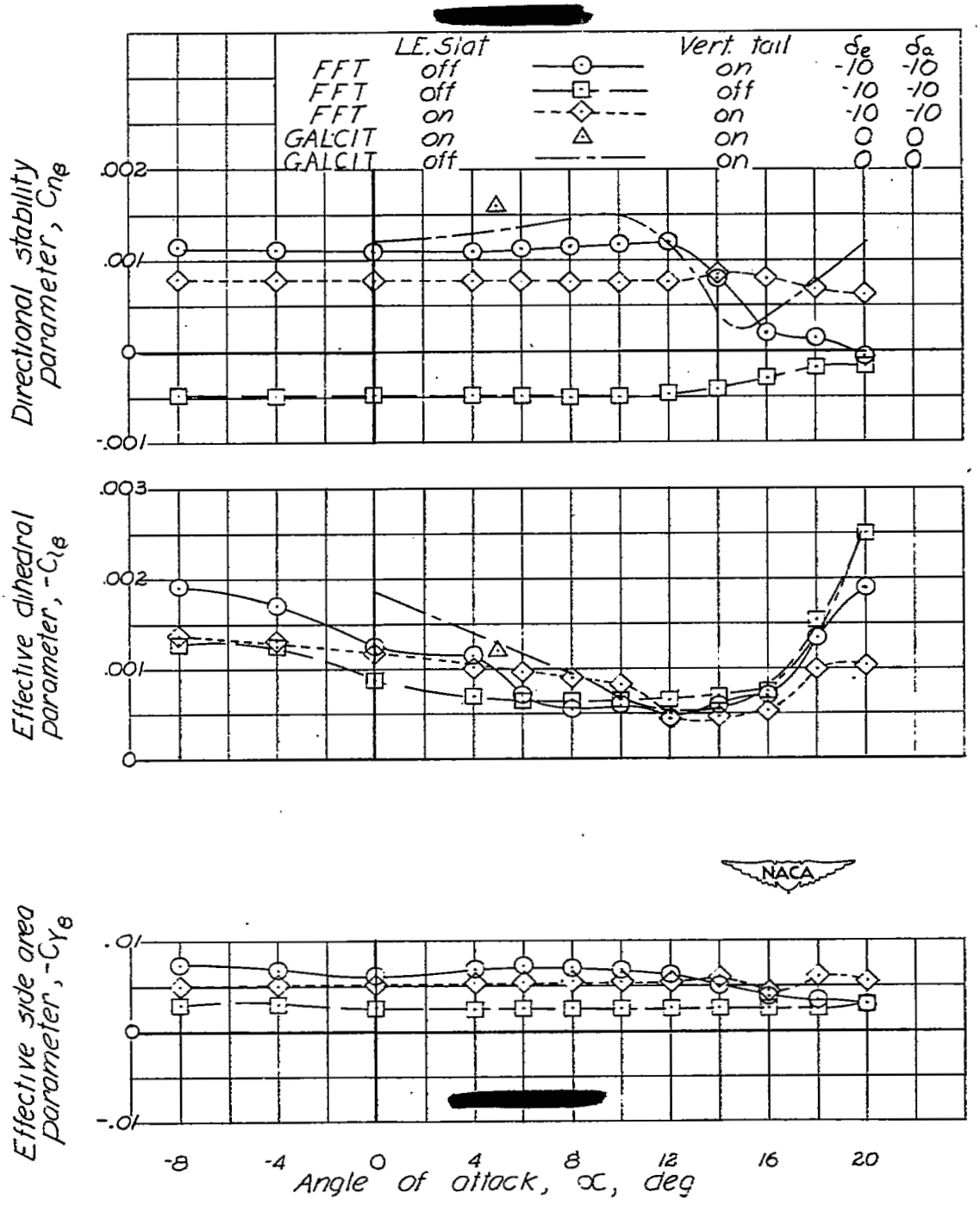

Figure 7.- Lateral stability characteristics of the $\frac{1}{20}$-scale free-flight-tunnel model of the Consolidated Vultee XB-53 airplane compared with the $\frac{1}{10}$-scale GALCIT model. Flaps retracted. GALCIT data from reference 3.

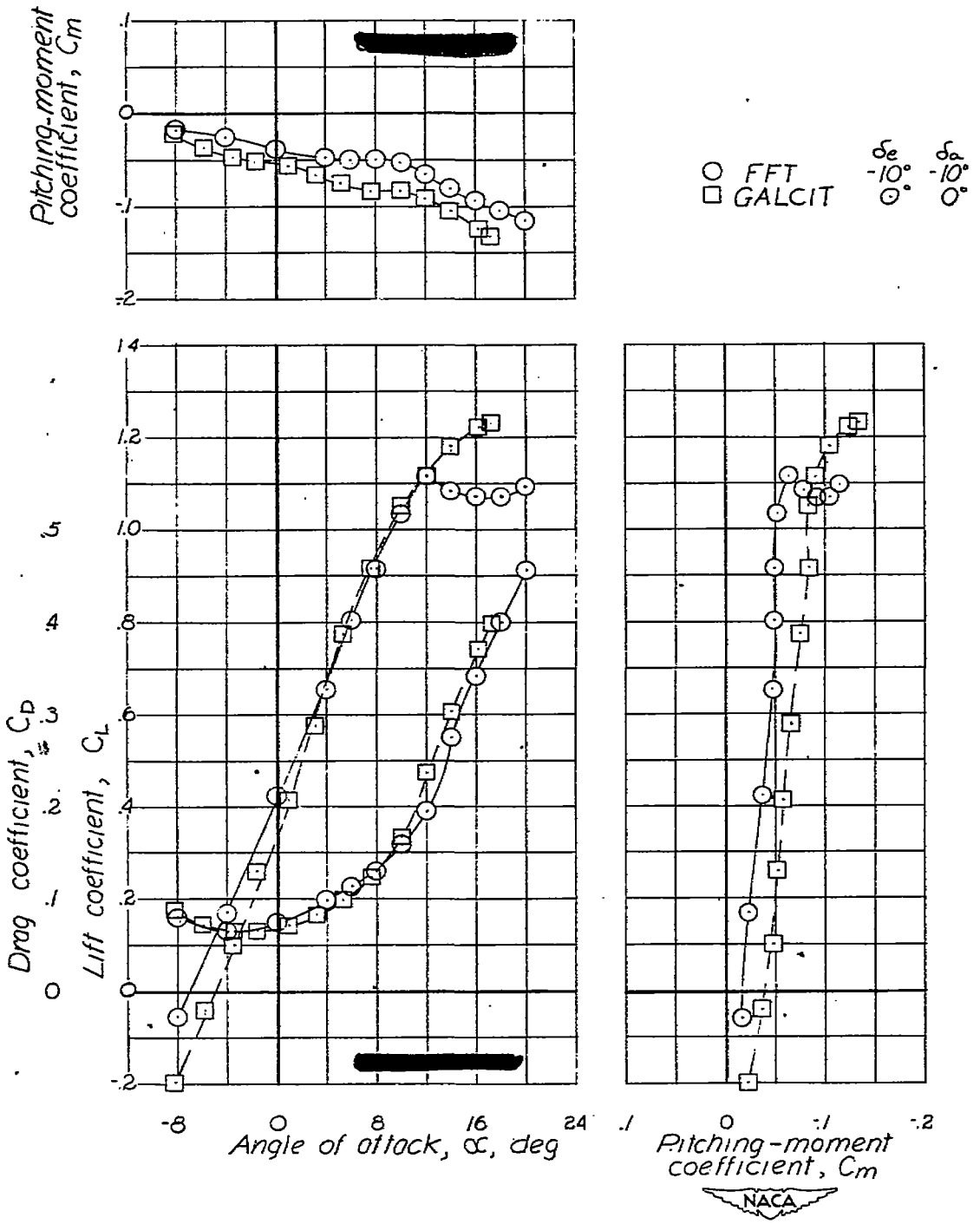

Figure 8.- Lift, drag, and pitching-moment characteristics of the $\frac{1}{20}$-scale free-flight-tunnel model of the Consolidated Vultee XB-53 airplane compared with the $\frac{1}{10}$-scale GALCIT model. Flaps extended. GALCIT data from reference 3. Leading-edge slat deflected.

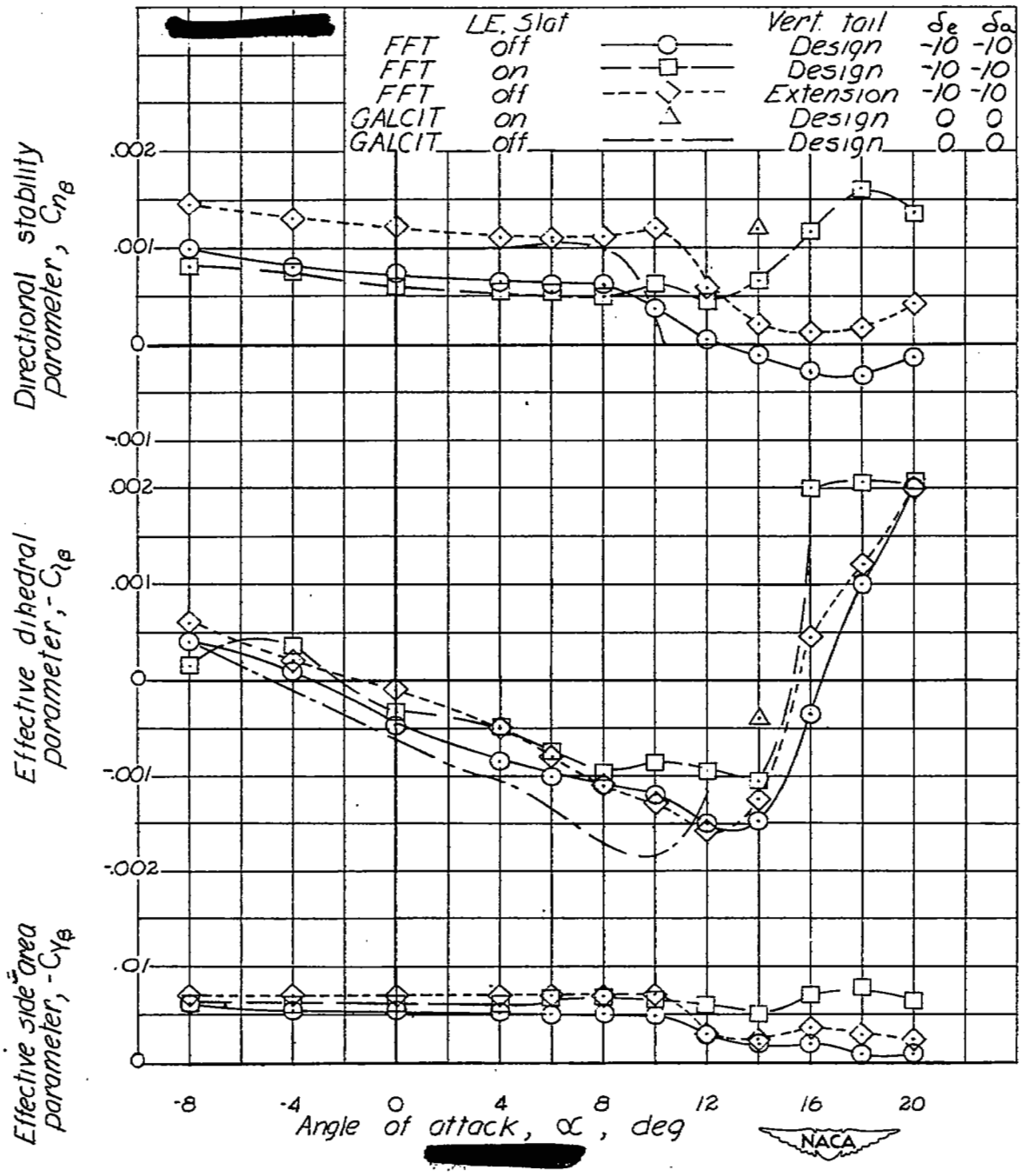

Figure 9:- Lateral stability characteristics of the $\frac{1}{20}$-scale free-flight model of the Consolidated Vultee XB-53 airplane compared with the $\frac{1}{10}$-scale GALCIT model. Flaps extended. GALCIT data from reference 3.

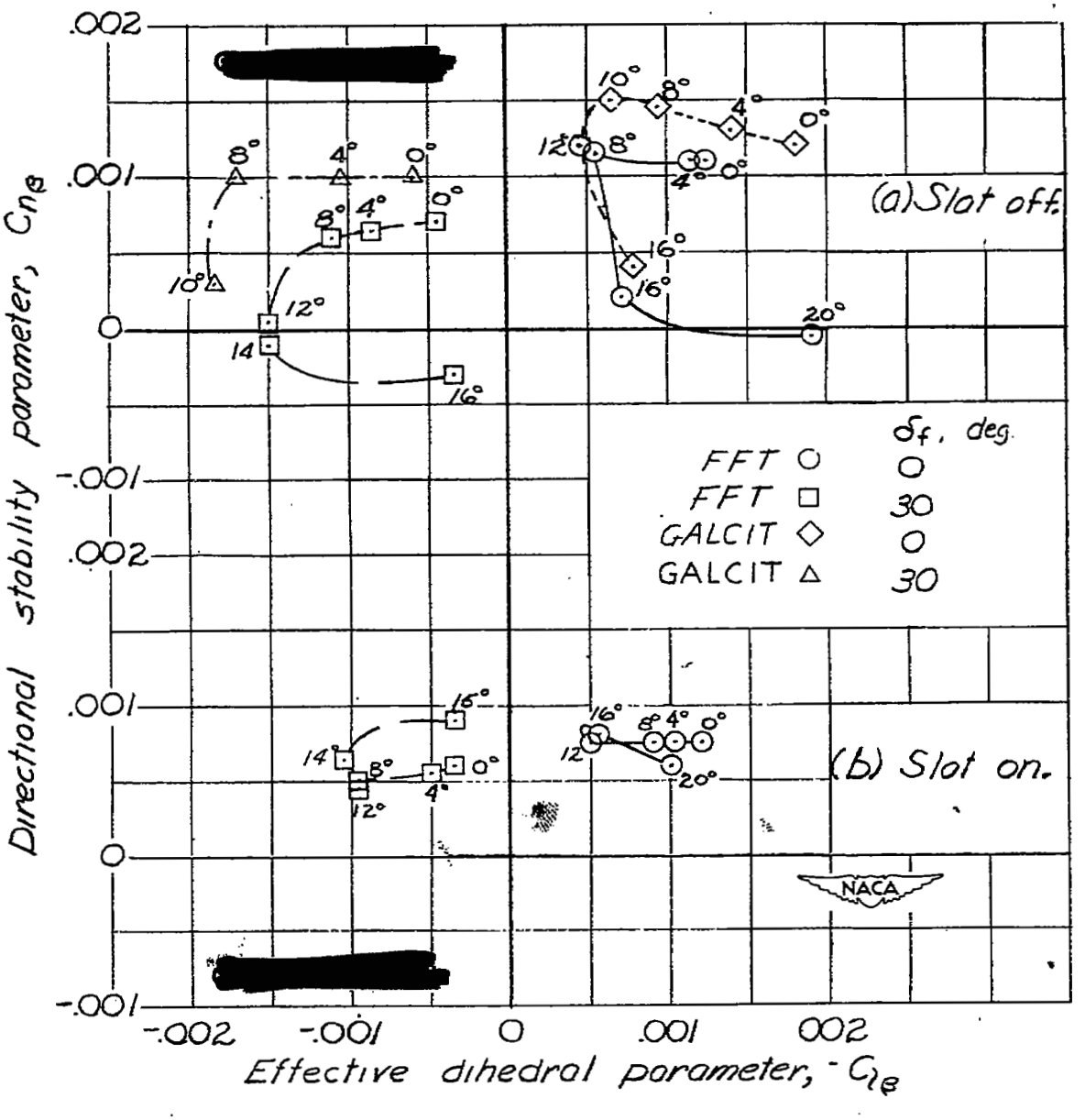

Figure 10.- Lateral stability charts for the Langley free-flight tunnel and GALCIT models of the XB-53 airplane. Design vertical tail.

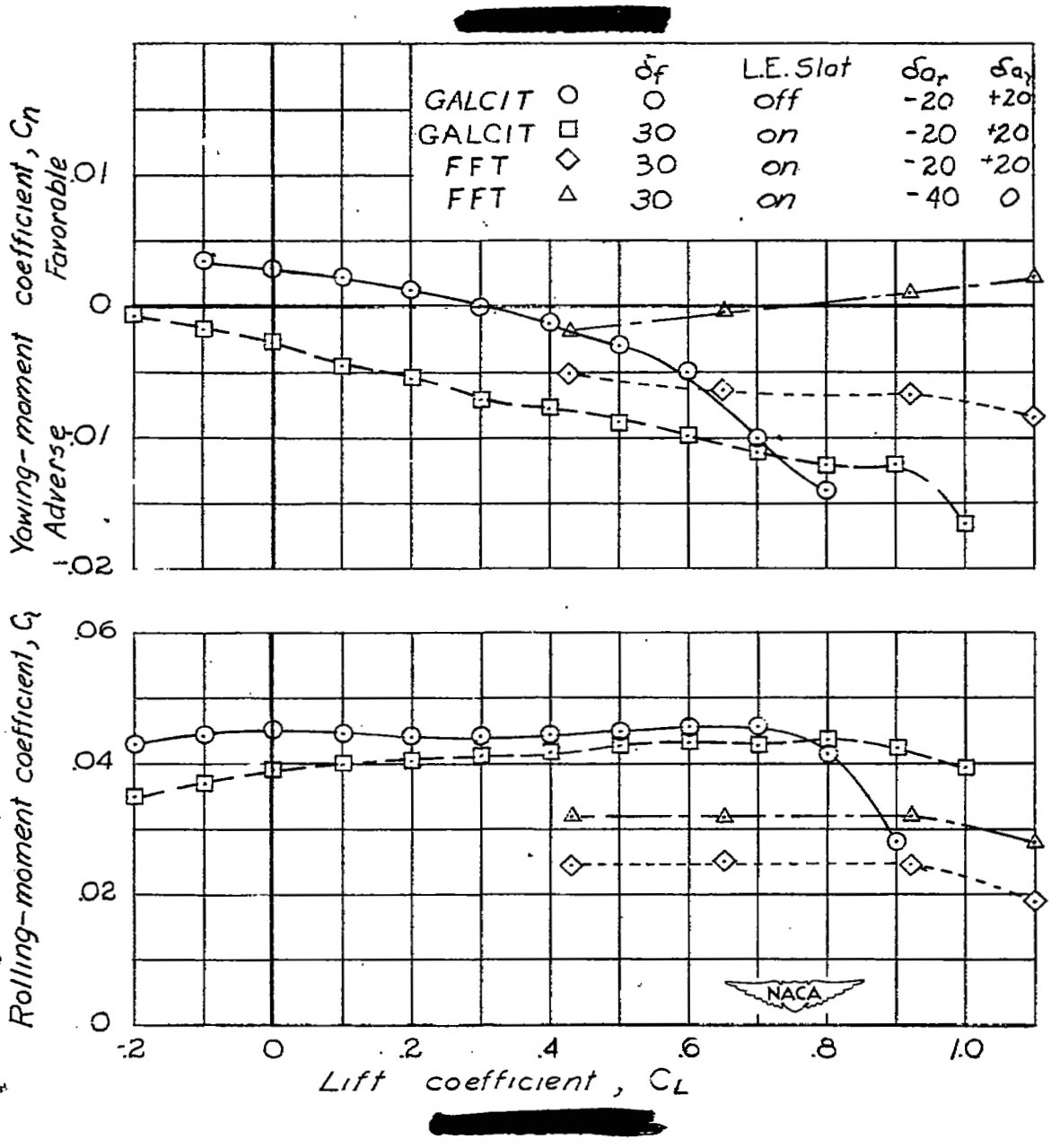

Figure 11.- Aileron rolling and yawing effectiveness of the $\frac{1}{20}$-scale free-flight-tunnel model of the Consolidated Vultee XB-53 airplane compared with the $\frac{1}{10}$-scale GALCIT model of reference 3.